# N-derivatives of peri-substituted dichalcogenide[FeFe]-hydrogenase mimics

Figliola, Carlotta; Male, Louise; Horswell, Sarah L; Grainger, Richard S

*DOI:*
10.1002/ejic.201500355



*Document Version*
Publisher's PDF, also known as Version of record

EurJIC European Journal of Inorganic Chemistry

ChemPubSoc Europe

FULL PAPER

DOI:10.1002/ejic.201500355

# *N*-Derivatives of *peri*-Substituted Dichalcogenide [FeFe]-Hydrogenase Mimics: Towards Photocatalytic Dyads for Hydrogen Production

**Carlotta Figliola,[a] Louise Male,[a] Sarah L. Horswell,*[a] and Richard S. Grainger*[a]**

**Keywords:** Photocatalysis / Electrocatalysis / Cyclic voltammetry / Porphyrinoids / Carbonyl ligands

Synthetic strategies towards molecular dyads based on *peri*-substituted dichalcogenide (S,Se) [FeFe]-hydrogenase synthetic mimics covalently linked to a ZnTPP photosensitizer are described. Dithiolate and diselenolate model systems **2**–**5** are prepared through condensation of 2-naphthaldehydes with *p*-methoxyaniline, reduction of the resulting Schiff base and oxidative insertion of $Fe_2(CO)_6$ into the dichalcogen bond of the imine or amine. Diselenolate-based [FeFe] complexes (imine **3** and amine **5**) are more efficient in electrocatalysis of proton reduction than their sulfur analogues **2** and **4** with increasing concentrations of *p*TsOH. Molecular dyad **1** containing a *peri*-substituted naphthalene dithiolate $Fe_2(CO)_6$ cluster covalently linked via an amine to ZnTPP is prepared through sequential zinc insertion into the porphyrin followed by iron insertion into the disulfide bond.

## Introduction

In the effort of developing renewable energy sources, great interest has been directed towards hydrogen[1] production by electrochemical and photochemical splitting of water.[2] Platinum complexes and colloids are commonly used to catalyse this reaction;[3] alternatively, complexes of cobalt,[4] nickel,[5] molybdenum[6] and, particularly, iron,[7] have been intensively studied.

Dithiolate-based [FeFe] complexes, $(\mu\text{-SR})_2Fe_2CO_{6-x}L_x$, are biomimics of the active site of the [FeFe]-hydrogenase enzyme, for which the rate of hydrogen production is the highest (6,000–9,000 $s^{-1}$)[8] among the known hydrogenases.[9] Since the first crystal structures of [FeFe]-hydrogenase,[10] variation of the organic backbone (R) and the use of electron-donating ligands (L) allowed achievement of remarkable progress in reproducing the enzyme's catalytic activity.[11] Recently we have reported a study on the contribution of aromatic backbones and chalcogens (SS, SeSe and SSe) to the redox properties of the [FeFe]-cluster.[12] As previously suggested,[13] the use of *peri*-substituted naphthalene and phenanthrene dichalcogen ligands allowed stabilisation of the catalytic intermediates and hence promoted hydrogen production. Furthermore, [FeFe]-hydrogenase analogues containing selenium[14] were confirmed to be more active towards proton reduction catalysis than their sulfur-based counterparts.

[FeFe]-hydrogenase synthetic mimics as catalysts for hydrogen production have also been investigated in photochemical systems.[15] Molecular dyads/triads, self-assemblies and bimolecular systems are the main strategies applied to design active catalysts for light-induced hydrogen production.[15e] Related to the current work, Wasielewski reported molecular dyads and triads containing *peri*-substituted [FeFe] complexes covalently attached to the photosensitiser ZnTPP, via an imide at the 4- and 5-positions of the naphthalene, for light-induced hydrogen production.[16] The turnover number of hydrogen generated was 0.56, along with decomposition of the [FeFe]-cluster.

Following our interest in the chemistry of *peri*-substituted dichalcogenides[17,18] and in the development of new and efficient [FeFe]-hydrogenase analogues,[12] we herein report the synthesis of ZnTTP-containing molecular dyad **1** and related imine/amine-substituted naphthalene-based [FeFe] complexes **2**–**5** (Figure 1). As for the enzyme's active site,[19] nitrogen-containing linkers, proximal to the [FeFe]-cluster, have been chosen since they are protonated upon acid addition and, hence, provide the metallic centre with

[a] School of Chemistry, University of Birmingham, Edgbaston, Birmingham B15 2TT, United Kingdom
E-mail: s.l.horswell@bham.ac.uk
r.s.grainger@bham.ac.uk
http://www.birmingham.ac.uk/staff/profiles/chemistry/horswell-sarah.aspx
http://www.birmingham.ac.uk/staff/profiles/chemistry/grainger-richard.aspx

Supporting information for this article is available on the WWW under http://dx.doi.org/10.1002/ejic.201500355.

protons.[11e] Spectroscopic and electrochemical properties of simple model systems **2**–**5** are reported and used for the initial studies into the synthesis of **1** as a potential catalyst for photocatalytic hydrogen production.

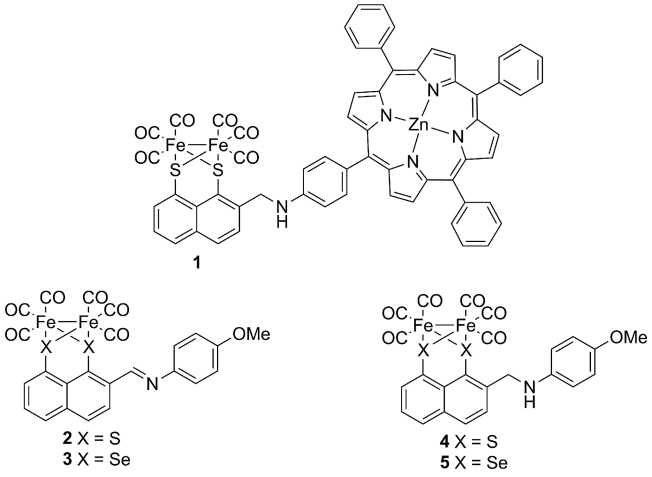


Figure 1. Molecular dyad **1** and imine/amine-substituted naphthalene-based [FeFe] complexes **2**–**5**.

## Results and Discussion

### Synthesis

The syntheses of model systems **2**–**5** are shown in Scheme 1. Refluxing 2-formyl-naphthalene 1,8-dithiole **6**[20] with a large excess of *p*-methoxyaniline in dry $CH_3CN$ gave the Schiff base **8** in excellent yield.[21] The known diselenole **7**[21] was converted to imine **9** using $TiCl_4$ as a catalyst and an excess of $NEt_3$.[22] [FeFe] complexes **2** and **3** were prepared through oxidative insertion of $Fe^0$ into the dichalcogen bond by treating **8** or **9** with $Fe_3(CO)_{12}$ in refluxing toluene and were sufficiently stable for isolation by column chromatography. Reduction of the imine double bond of **8** and **9** with a large excess of $NaBH_4$[21] generated the corresponding amines which were reacted directly with $Fe_3(CO)_{12}$ to yield the novel [FeFe] complexes **4** and **5**.[12,23]

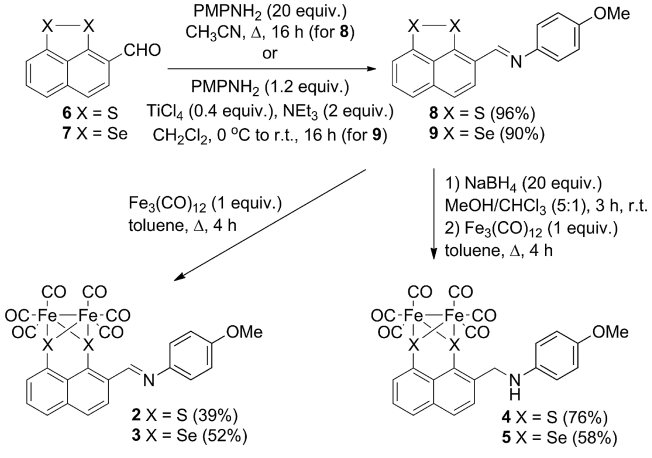


Scheme 1. Synthesis of [FeFe] complexes **2**–**5**.

Based on the synthesis of **2** and **3**, we attempted to synthesise molecular dyads containing an imine-linker between the photosensitizer (porphyrin) and the catalyst ([FeFe] complex). Reaction of tetraphenylporphyrin-amine ($TPPNH_2$) **10**[24–26] with $Zn(OAc)_2$ in refluxing pyridine followed by further reaction of the resulting $ZnTPPNH_2$[27] with aldehyde **6** or **7**, using a further excess of $Zn(OAc)_2$,[16a] gave the zinc-containing Schiff bases **11** and **12** in good to excellent yields. Following the synthetic sequence described for [FeFe] complexes **2** and **3**, **11** and **12** were treated with $Fe_3(CO)_{12}$ in refluxing toluene to afford the corresponding [FeFe] complexes (not shown); however, these were prone to degradation upon attempted column chromatography, with $^1H$ NMR spectroscopy and mass spectrometry showing both the formation of the expected [FeFe] complexes and the presence of the starting aldehyde (**6** or **7**) and $ZnTPPNH_2$.

Reduction of the imine double bond in **11** and **12** could not be achieved in an analogous manner to **8** and **9**.[21] Consequently, aldehydes **6** and **7** were treated with **10** in refluxing toluene in the presence of catalytic $La(OTf)_3$[28] to afford imines **13** and **14** in high yields. Reduction of imine **13** to amine **15** was successfully achieved using $NaBH_3CN$ and catalytic amounts of AcOH.[29] Metallation of the porphyrin core with $Zn(OAc)_2$ followed by oxidative insertion into the S–S bond of the naphthalene-1,8-dithiole gave the target [FeFe] complex **1** (Scheme 2). In contrast, attempts to reduce the double bond of diselenole **14** were unsuccessful. $NaBH_4$[21] caused degradation of **14**, whereas $NaBH_3CN$,[29] $NaBH(OAc)_3$[30] as well as hydrogenation[31] only resulted in recovered starting material. Consequently, the synthesis of the selenium-containing molecular dyad corresponding to **1** could not be achieved.

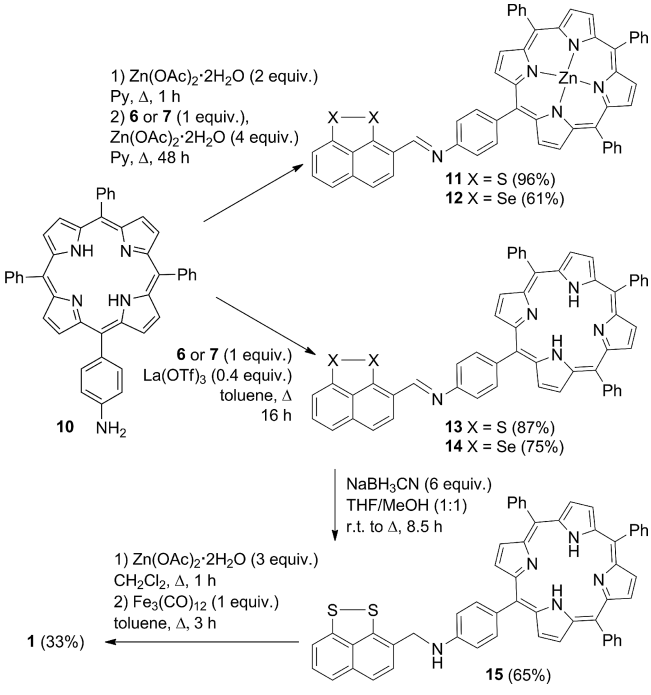


Scheme 2. Synthesis of molecular dyad **1**.

### Spectroscopic and Electrochemical Analysis of [FeFe] Complexes 2–5

[FeFe] complexes **2**–**5** were characterised by $^{1}H$, $^{13}C$ NMR, IR and UV/Vis spectroscopy. Molecular structures of [FeFe] complexes **2** and **4** were also confirmed by X-ray diffraction.

$^{1}H$ NMR spectra of **2**–**5** displayed the expected downfield shift of the aromatic protons compared with those of the corresponding ligands **8** and **9** associated with the insertion of the [FeFe]-cluster into the dichalcogen bond.[12] $^{13}C$ NMR spectra showed one single peak at 207 or 208 ppm, assigned to the carbonyl ligands binding the iron centre in the dithiolate and diselenolate-bridged complexes, respectively.[12]

The IR stretching wavenumbers of the carbonyl ligands are listed in Table 1. As previously observed for related $Fe_2CO_6$ complexes with aromatic dichalcogen ligands,[12,13a,13b,13f,13m] the absorption bands are all in the range 2070–1950 $cm^{-1}$. [FeFe] complexes **3** and **5** display a bathochromic shift of the carbonyl stretching compared with the analogous dithiolate-based **2** and **4**, confirming what has been previously observed.[12]

Table 1. Carbonyl IR stretches of [FeFe] complexes **2**–**5**.

| | $\tilde{\nu}$ (CO) [$cm^{-1}$] |
|---|---|
| **2** (SS) | 2066, 2024, 1977, 1959 |
| **3** (SeSe) | 2061, 2024, 1978, 1953 |
| **4** (SS) | 2064, 2026, 2005, 1988, 1963 |
| **5** (SeSe) | 2057, 2020, 1997, 1981, 1958 |

The UV/Vis spectra of the [FeFe] complexes and the corresponding values for the extinction coefficient are reported in Figure S1 and Table S2, respectively (Supporting Information).

The UV/Vis spectra of amine-substituted [FeFe] complexes **4** and **5** display intense bands in the range 210–260 nm, which are assigned to the naphthalene π-π* transition. The iron-carbonyls metal-ligand charge transfer (MLCT) or ligand-metal charge transfer (LMCT) absorbs in the range 310–410 nm, consistent with previous measurements.[12,13g,13m,32] Additionally, a weak absorption band is observed in the range 410–510 nm, which corresponds to the metal d-d transition.[12,13g,13m,32] Imine-substituted [FeFe] complexes **2** and **3** display a continuous absorption in the range 250–400 nm, due to the highly conjugated system. The iron d-d transitions of **2** and **3** are stronger than those recorded for the corresponding **4** and **5**.

Molecular structures of [FeFe] complexes **2** and **4** were confirmed by X-ray analysis.[33] Crystal structures of **2** and **4** are shown in Figure 2; bond lengths and angles are listed in Table 2. Crystal data and structure refinement details are described in Table S4 (Supporting Information).

Both amine and imine-substituted complexes possess a dithiolate-bridged [FeFe]-core which assumes the typical butterfly architecture with two iron centres linked to three carbonyl ligands in a distorted square-pyramidal geometry.[12,13f] The Fe–Fe bond length for each complex is comparable with those reported for the active site of [FeFe]-hydrogenase (2.6 Å), as is the bond length between each iron and sulfur (Fe1–S1 = Fe1–S2 = Fe2–S2 = Fe2–S2 = 2.3 Å in the enzyme).[10]

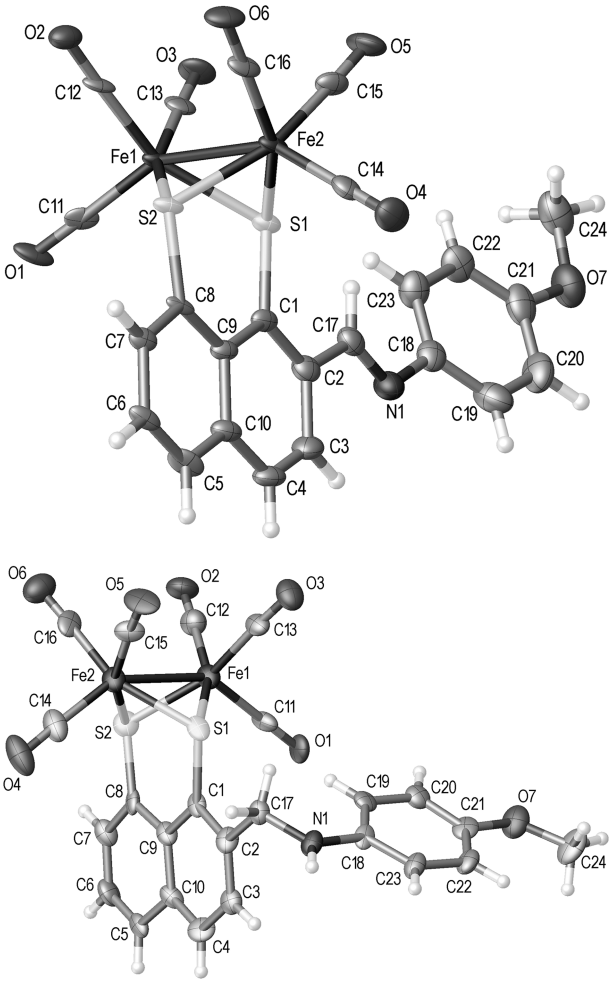


Figure 2. Molecular structures of [FeFe] complexes **2** (top) and **4** (bottom) with ellipsoids drawn at the 50% probability level. The structure of **2** contains two crystallographically-independent molecules of which only one (molecule 1) is shown.

The presence of an imino- or amino-group in position 2 on the naphthalene ring of **2** and **4** does not change the general structure of the complexes, which are comparable in bond lengths and angles with the data reported for similar compounds.[12,13f] The crystal structure of **2** contains two crystallographically-independent molecules, which are comparable in geometry. In both molecules the structure displays a *trans* geometry of the imine double bond. The phenyl substituent on the nitrogen is outside of the plane of the conjugated system by rotation around the N(1)–C(18) bond [torsion angles: C(23)–C(18)–N(1)–C(17) = –25.7(14)° and C(19)–C(18)–N(1)–C(17) = 155.4(9)°] in molecule 1 and C(123)–C(118)–N(101)–C(117) = 35(2)° and C(119)–C(118)–N(101)–C(117) = –146.3(14)° in molecule 2, Table 2 and Table S3 in Supporting Information.

The electrochemical properties of the amine and imine-substituted [FeFe] complexes **2**–**5** were investigated by cyclic voltammetry. Based on our previous studies,[12] all the mea-

 

Table 2. Selected bond lengths [Å] and angles [°] for compounds **2** (molecule 1 only) and **4**. For geometry of molecule 2 of compound **2** see Supplorting Information, Table S3.

| | **2** | **4** |
|---|---|---|
| Fe(1)–Fe(2) | 2.5094(16) | 2.545(4) |
| Fe(1)–S(1) | 2.249(2) | 2.261(6) |
| Fe(1)–S(2) | 2.243(2) | 2.236(6) |
| Fe(2)–S(1) | 2.245(2) | 2.271(6) |
| Fe(2)–S(2) | 2.239(2) | 2.241(5) |
| Fe(1)–C(11) | 1.798(9) | 1.83(2) |
| Fe(1)–C(12) | 1.810(9) | 1.79(2) |
| Fe(1)–C(13) | 1.806(9) | 1.83(2) |
| Fe(2)–C(14) | 1.804(10) | 1.81(2) |
| Fe(2)–C(15) | 1.796(9) | 1.820(19) |
| Fe(2)–C(16) | 1.816(10) | 1.81(2) |
| S(1)–C(1) | 1.769(8) | 1.754(18) |
| S(2)–C(8) | 1.773(8) | 1.77(2) |
| S(1)–Fe(1)–S(2) | 83.84(8) | 84.3(2) |
| S(1)–Fe(2)–S(2) | 84.00(8) | 84.0(2) |
| S(1)–C(1)–C(9) | 123.8(6) | 124.3(15) |
| S(2)–C(8)–C(9) | 126.3(6) | 128.1(14) |
| C(8)–C(9)–C(1) | 124.9(7) | 122.8(16) |
| C(1)–C(2)–C(17)–N(1) | 179.0(8) | –146.0(18) |
| C(3)–C(2)–C(17)–N(1) | 0.8 (13) | 33(2) |
| C(19)–C(18)–N(1)–C(17) | 155.4(9) | –2(2) |
| C(23)–C(18)–N(1)–C(17) | –25.7(14) | 177.9(16) |

surements were recorded in $CH_3CN$ at room temperature, using a three electrode-cell with glassy carbon as working electrode, $Ag/AgNO_3$ as reference electrode, and platinum as counter electrode. All the potentials were measured with respect to the ferrocene redox couple ($Fc/Fc^+$), which was used as internal reference. All the peak potentials and the corresponding half-wave potentials ($E_{1/2}$) are listed in Table 3 and cyclic voltammograms are shown in Figure 3.

Table 3. Electrochemical reduction potentials (vs. $Fc/Fc^+$) of [FeFe] complexes **2**–**5** (1 mM) in 0.1 M $NBu_4PF_6/CH_3CN$ at 0.01 V $s^{-1}$ scan rate.

| | **2** (SS) | **3** (SeSe) | **4** (SS) | **5** (SeSe) |
|---|---|---|---|---|
| $E'_{pc}$ (V) | –1.51 | –1.45 | –1.51 | –1.51 |
| $E'_{1/2}$ (V)[a] | –1.44 | –1.41 | –1.62 | –1.41 |
| $E''_{pc}$ (V) | –1.74 | –1.86 | –1.85 | –1.90 |
| $E''_{1/2}$ (V)[b] | – | –1.81 | –1.78 | – |
| $E_{pa}$ (V) | 1.00 | 0.96 | 0.46 | 0.52 |
| | | | 0.76 | 0.68 |
| $E_{1/2}$–$E°_{HA}$[c] (V) | 0.80 | 0.76 | 0.96 | 0.76 |

[a] $Fe^IFe^I \rightarrow Fe^IFe^0$. [b] $Fe^IFe^0 \rightarrow Fe^0Fe^0$. [c] $E°_{pTsOH}$ = –0.65 V (vs. $Fc/Fc^+$) in $CH_3CN$ at room temperature.[34]

All complexes undergo two one-electron reductions, which are assigned to $Fe^IFe^I$–$Fe^0Fe^I$ and $Fe^0Fe^I$–$Fe^0Fe^0$, by analogy with previously reported [FeFe] complexes.[12] In addition, each [FeFe] complex shows one or two one-electron oxidations, corresponding to $Fe^IFe^I$–$Fe^{II}Fe^I$ and $Fe^{II}Fe^I$–$Fe^{II}Fe^{II}$, respectively.[12] The first and the second reduction event result in a chemical decomposition (EC reaction), which reduces the amplitude of the return wave. This rearrangement is unlikely to involve fragmentation of the backbone because an oxidation peak is observed on the return sweep.[13f,13g] In the case of [FeFe] complex **4**, the peak separation of the first and the second reduction waves is

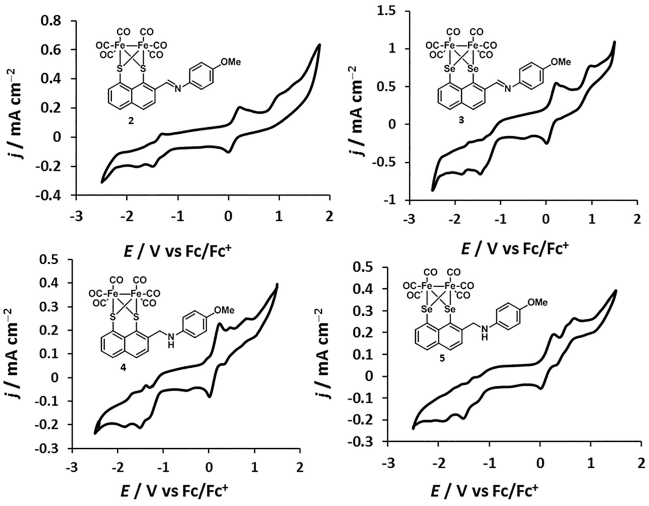


Figure 3. Cyclic voltammograms for [FeFe] complexes **2**–**5** (1 mM) in 0.1 M $NBu_4PF_6/CH_3CN$ at 0.01 V $s^{-1}$ scan rate.

similar to that observed for the $Fc/Fc^+$ internal redox couple, indicating reversible behaviour (fast electron transfer kinetics). In contrast, [FeFe] complexes **2**, **3** and **5** displayed a weak oxidation peak on the return sweep, presumably meaning decomposition of the reduced product. The same observation can be made for the oxidation processes (except for the first oxidation of **4** and **5**).

The first reduction wave of selenium-based [FeFe] complexes **3** and **5** occurs at less negative potential than the corresponding sulfur counterpart **2** and **4** (**3** and **5**: $E_{1/2}$ = –1.41 V vs. **2** and **4**: $E_{1/2}$ = –1.44 V and –1.62 V, respectively) (Table 3), consistent with previous analyses.[12] However, the presence of selenium might affect the stability of both reduced products, compared with the analogous sulfur-based complex. The amine-substituted dithiolate **4** is shown to be the most thermodynamically stable among the reported complexes, since both reductions are reversible (Figure 3).

[FeFe] complexes **2**–**5** were investigated as proton reduction catalysts by monitoring their electrochemical properties upon addition of *p*TsOH (concentration 0.5 mM to 10 mM).[12] Cyclic voltammograms are shown in Figure 4 and Figure S5 (Supporting Information).

Imines **2** and **3** show the first reduction process shifted at less negative potentials than those recorded in the absence of acid (Table 3). Notably, the first reduction wave moves cathodically from –0.7 V to –1.1 V (**2**) and from –0.5 V to –1.17 V (**3**), upon increasing the acid concentration from 0.5 mM to 5 mM. At higher concentration of acid (7.5 mM and 10 mM) this reduction wave becomes negligible. The shift in peak position of this first reduction process is independent of the acid concentration; however, the peak current increases linearly with the acid concentration. Upon increasing the concentration of *p*TsOH (from 0.5 to 2 mM), the second and the third reduction waves are slightly shifted towards more negative potentials. At higher concentration of acid, they are notably shifted towards more negative potentials and the peak current is significantly increased.[12]

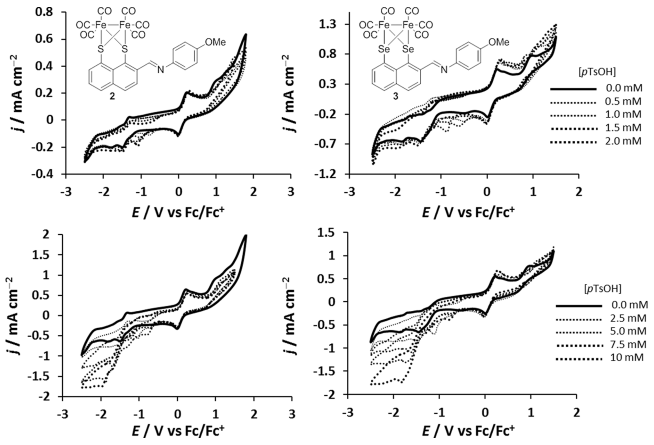


Figure 4. Cyclic voltammograms for [FeFe] complexes **2** and **3** (1 mM) in 0.1 M $NBu_4PF_6/CH_3CN$ at 0.01 $Vs^{-1}$ scan rate with increasing concentrations of *p*TsOH from 0.5 mM to 2 mM (upper graphs) and from 2.5 mM to 10 mM (lower graphs).

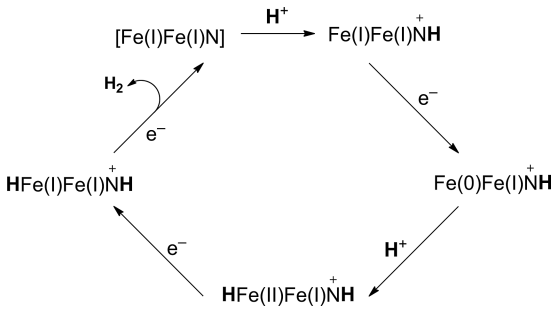


Scheme 3. Proposed mechanism for the proton reduction catalysis by [FeFe] complexes **2** and **3** in the presence of *p*TsOH.

The first reduction peak of the amines **4** and **5** is shifted in the range from –0.5 V to –0.6 V only upon addition of 0.5 and 1 mM of *p*TsOH. This process is less defined than in the imine-substituted **2** and **3**. At high concentration of acid, the second and the third reduction process follow what has been described previously for complexes **2** and **3**.

As previously observed,[35–37] the first process may involve the reduction of the protonated [FeFe] complexes **2**–**5** upon addition of *p*TsOH. The introduction of a positive charge could explain the shift towards more positive potential compared with that recorded in the absence of acid. Protonation of the amino/imino substituent, proximal to the [FeFe]-cluster, is thought to decrease the activation energy of the Fe–H bond formation; hence, it favours proton reduction catalysis.[35–37] Protonation of complexes **2** and **3** is shown to occur at both low and high acid concentration, while for the amine equivalent **4** and **5** only at low concentration of *p*TsOH.

The proposed mechanism for the proton reduction catalysis of [FeFe] complexes **2** and **3** is shown in Scheme 3. Upon addition of *p*TsOH, $[Fe^IFe^IN]$ is protonated to $[Fe^IFe^INH]^+$, which could explain the anodic shift of the first reduction potential and give $[Fe^0Fe^INH]^+$. This species reacts again with acid to generate $[HFe^{II}Fe^INH]^+$, which, after two more one-electron reductions, liberates hydrogen and regenerates the initial $[Fe^IFe^IN]$.[35,37] Amine-substituted [FeFe] complexes **4** and **5** follow the above mechanism at low acid concentration. At high concentration of acid, they follow the proton reduction mechanism described for similar naphthalene-based [FeFe] complexes.[12,13f]

The efficiency of proton reduction catalysis of [FeFe] complexes **2**–**5** was evaluated in terms of $E_{1/2}$-$E°_{HA}$,[12] which gives a measure of the overpotential for the acid reduction to occur in the presence of the catalyst. Table 3 reports the values of **2**–**5** for *p*TsOH reduction. Diselenolate-bridged [FeFe] complexes show lower values than their sulfur counterparts, suggesting they are more efficient catalysts towards proton reduction. This is consistent with the literature[14] and with previous results.[12] The catalytic efficiency of [FeFe] complexes **2**–**5** was also estimated in terms of peak current increase (Figure S8, Supporting Information).[12] Only high concentrations of acid were considered, since the peak height is more markedly affected than at low concentration. Diselenolate-based [FeFe] complexes **3** and **5** give a bigger peak current increase than the equivalent dithiolates **2** and **4**, but this effect is less predictable than that observed for previously reported complexes.[12]

## Spectroscopic and Electrochemical Analysis of Molecular Dyad 1

Following spectroscopic and electrochemical analysis of [FeFe] complex **4**, molecular dyad **1** was analysed by $^1H$ and $^{13}C$ NMR, IR, UV/Vis and emission spectroscopy. The $^1H$ NMR spectrum displayed a significant downfield shift of naphthalene and amino-linker peaks of **1** compared with those of the ligand **15**, associated with the insertion of the [FeFe]-cluster. The $^{13}C$ NMR spectrum showed the characteristic peak for the carbonyls of the [FeFe]-cluster at $\delta$ = 207 ppm.

IR spectroscopy displayed three stretching bands at 2072, 2032 and 1982 $cm^{-1}$, which are assigned to the iron-bound carbonyl ligands.[16] [FeFe] complexes **4** (Table 1) and **1** showed comparable wavenumbers for the carbonyl stretching, suggesting that ZnTPP in the ground state does not significantly affect the [FeFe]-cluster.[16a]

The UV/Vis absorption spectrum of **1** in Figure S3 (Supporting Information) shows one intense Soret band at 422 nm and two weak Q bands at 550 nm and 593 nm, respectively.[38] By analogy with the model system **4** (Table S2 and Figure S1 in Supporting Information), the absorption band at 254 nm is assigned to the first naphthalene π-π* transition and those at 308 nm and 355 nm are assigned to the iron-carbonyls MLTC or LMCT.

In order to establish if the electron transfer is a thermodynamically feasible process, a cyclic voltammogram of **1** was recorded in $CH_2Cl_2/CH_3CN$ (7:3) using the same system set up for the analysis of **4** (Figure 5). It displays two reduction waves at –1.72 V and –2.05 V ($E'_{1/2}$ = –1.65 V and $E''_{1/2}$ = –1.94 V), which are assigned to $Fe^IFe^I$–$Fe^0Fe^I$ and $Fe^0Fe^I$–$Fe^0Fe^0$, respectively, by analogy with [FeFe]

 

complex **4**. Two oxidation waves are also shown at 0.4 V and 0.7 V, which are attributed to $Fe^{I}Fe^{I}$–$Fe^{II}Fe^{I}$ and $Fe^{II}Fe^{I}$–$Fe^{II}Fe^{II}$, respectively.

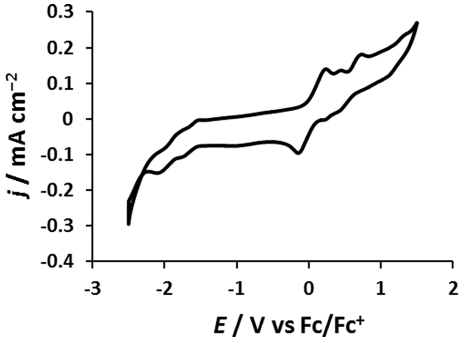


Figure 5. Cyclic voltammogram of complex **1** (1 mM) in 0.1 M $NBu_4PF_6/CH_2Cl_2/CH_3CN$ (7:3) at 0.01 V $s^{-1}$ scan rate.

The first reduction of molecular dyad **1** occurs at less negative potential ($E'_{1/2}$ = –1.65 V) than the oxidation of the excited species ZnTPP* (= –1.74 V).[15c] This suggests that the oxidative quenching of excited species ZnTPP* by the [FeFe]-cluster is thermodynamically favoured.[15] Furthermore, previous results on the catalytic proton reduction properties of **4**, along with the spectroscopic and electrochemical similarities between **4** and **1**, suggest that the reduced species of the [FeFe]-cluster in **1** is suitable for catalysing proton reduction and producing hydrogen.

## Conclusions

In this report we describe a new strategy to obtain [FeFe]-hydrogenase synthetic mimics stabilised by *peri*-substituted naphthalene dithiolate or diselenolate ligands which also contain basic nitrogen functionality in close proximity to the catalytically active site. [FeFe] complexes **2**–**5** have been shown to catalyse proton reduction. Protonation of the amino and imino groups under acidic conditions was detected with cyclic voltammetry. The synthetic strategy was extended to the preparation of a molecular dyad containing a tetraphenylporphyrinatozinc as a potential photosensitizer. Electrochemical studies indicate that electron transfer between the two moieties of **1** is thermodynamically feasible and consistent with the oxidative quenching of the excited ZnTPP* by the [FeFe]-cluster.

## Experimental Section

**General Experimental:** Solvents and reagents were purified as follows. *p*-Toluenesulfonic acid monohydrate was purchased from Aldrich, dehydrated by heating at 100 °C for 4 h under vacuum and recrystallised from $CHCl_3$.[40] Dry solvents were obtained and purified using a Pure Solv-MD solvent purification system and were transferred under argon. All other reagents and solvents were purchased and used as received from commercial sources. The following cooling baths were used: 0 °C (ice/water) and –78 °C (dry ice/acetone). All reactions in non-aqueous solvents were carried out under argon in oven-dried glassware. Melting points were determined using open glass capillaries on a Gallenkamp melting point apparatus and are uncorrected. Analytical TLC was carried out on Merck 60 F245 aluminium-backed silica gel plates. Short wave UV (245 nm) and $KMnO_4$ were used to visualise components. Compounds were purified by flash column chromatography using Merck silica gel 60.

Naphtho[1,8-*cd*][1,2]dithiole-3-carbaldehyde[20] (**6**), naphtho[1,8-*cd*][1,2]diselenole-3-carbaldehyde[21] (**7**), 5,10,15-triphenyl-20-(4-amino)phenylporphyrin[24–26] (**10**), zinc 5,10,15-triphenyl-20-(4-amino)phenylporphyrin[27] (**16**) were prepared according to literature procedures.

$^1H$ and $^{13}C$ NMR spectroscopic data were recorded on a Bruker AVIII300 (300 MHz $^1H$, $T$ = 293 K), Bruker AVIII400 (400 MHz $^1H$, 101 MHz $^{13}C$, $T$ = 293 K) or on a Bruker AV400 (400 MHz $^1H$, 101 MHz $^{13}C$, $T$ = 293 K) spectrometer. Spectra were recorded in $CD_2Cl_2$ referenced to residual $CH_2Cl_2$ ($^1H$, 5.33 ppm; $^{13}C$, 53.84 ppm), [$D_6$]DMSO referenced to residual DMSO ($^1H$, 2.50 ppm; $^{13}C$, 39.52 ppm) and $CDCl_3$ referenced to residual $CHCl_3$ ($^1H$, 7.26 ppm; $^{13}C$, 77.16 ppm).[41] Chemical shifts ($\delta$) are reported in ppm and coupling constants ($J$) are reported in Hz. The following abbreviations are used to describe multiplicity: s-singlet, d-doublet, t-triplet, q-quartet, *m*-multiplet, br-broad. All the reported coupling constants are averaged, when the coupling constants are close in value. Mass spectra (MS) were recorded on a Microwaters LCT TOF with a mixture (2:1) of MeOH and $CHCl_3$ as mobile phase, Microwaters SynaptG26 with mixture (2:1) of $CHCl_3$ and MeOH as mobile phase or on a Microwaters GCT Premier Probe, utilising electrospray ionisation (recorded in the positive mode), or electron impact ionisation, and both are reported as *m*/*z* (%) and they are given as $[M + H]^+$ and $M^+$. High resolution mass spectra (HRMS) were recorded on a Microwaters LCT TOF, Microwaters SynaptG26 or on Microwaters GCT Premier Probe using a leucine enkephalin-lock mass incorporated into the mobile phase. IR spectra were recorded neat on a Perkin–Elmer 100 FT-IR spectrometer.

UV/Vis spectra were recorded in a 1 mL quartz cuvette of 1 cm pathlength at 298 K on a CARY50 spectrometer. Wavelengths are given in nm, and extinction coefficients in $M^{-1} cm^{-1}$. Emission spectra were recorded on a Shimadzu RF-5301PC spectrophotometer with excitation and emission slit width both set at 10 nm and using 1 mL quartz cuvette of 1 cm pathlength; wavelengths are given in nm.

**$[Fe_2(CO)_6(1,8\text{-}S_2\text{-}2\text{-}CH_2\text{-}N\text{-}(ZnTPP)\text{-}C_{10}H_5)]$ (1):** To a solution of amine **15** (0.02 g, 0.02 mmol) in $CHCl_3$ (11 mL) $Zn(OAc)_2{\cdot}2H_2O$ (0.01 g, 0.06 mmol) was added in one portion at room temperature and the reaction mixture was heated under reflux for 1 h. After this time TLC analysis (7:3, $CH_2Cl_2$/hexane) indicated total consumption of **15**. The reaction mixture was cooled down to room temperature and the solvent evaporated under reduced pressure. The residue was dissolved in toluene (11 mL) and $Fe_3(CO)_{12}$ (0.01 g, 0.03 mmol) was added in one portion at room temperature and the reaction mixture was refluxed for 3 h under argon atmosphere. The solvent was removed under reduced pressure and the residue purified by column chromatography ($CH_2Cl_2$) to give complex **1** as a bright purple opaque solid (0.008 g, 33%). $R_f$ = 0.90 ($CH_2Cl_2$); m.p. > 300 °C. $\lambda_{nm}$ ($CH_2Cl_2$) = 254 ($\varepsilon = 5.8 \times 10^4$ $M^{-1} cm^{-1}$), 308 ($\varepsilon = 3.3 \times 10^4$ $M^{-1} cm^{-1}$), 355 ($\varepsilon = 3.5 \times 10^4$ $M^{-1} cm^{-1}$), 422 ($\varepsilon = 4.5 \times 10^5$ $M^{-1} cm^{-1}$), 550 ($\varepsilon = 2.6 \times 10^4$ $M^{-1} cm^{-1}$), 593 ($\varepsilon = 7.3 \times 10^3$ $M^{-1} cm^{-1}$). IR (solid neat, ATR): $\tilde{\nu}_{max}$ = 3413, 3051, 3021, 2922, 2852, 2072 (CO), 2032 (CO), 1982 (CO), 1596, 1519, 1485, 1440, 1339, 1205, 1179, 1069, 993, 831, 795, 749, 718, 699 $cm^{-1}$. $^1H$ NMR (400 MHz, $CDCl_3$): $\delta$ = 4.83 (s, 2 H, $CH_2$), 6.67 (d, $J$ = 7.7 Hz, 2

 

H, Ar*H*), 7.39 (t, *J* = 7.6 Hz, 1 H, Ar*H*), 7.69 (d, *J* = 8.6 Hz, 1 H, Ar*H*), 7.71–7.79 (m, 9 H, Ar*H*), 7.94 (d, *J* = 7.7 Hz, 2 H, Ar*H*), 7.99 (d, *J* = 7.8 Hz, 2 H, Ar*H*), 8.22 (d, *J* = 6.3 Hz, 6 H, Ar*H*), 8.27 (d, *J* = 7.2 Hz, 1 H, Ar*H*), 8.85–9.03 (m, 8 H, Ar*H*); $^{13}$C NMR (101 MHz, $CDCl_3$): 48.4 ($CH_2$), 111.5 (2× CH), 120.9 (C), 121.1 (2× C), 121.9 (C), 123.3 (C), 124.8 (C), 125.2 (CH), 126.7 (6× CH), 127.1 (CH), 127.6 (3× CH), 131.4 (CH), 131.9 (2× CH), 132.0 (4× CH), 132.0 (2× CH), 132.4 (CH), 132.8 (C), 133.3 (CH), 133.9 (2× C), 134.6 (6× CH), 135.6 (2× CH), 143.1 (3× C), 143.3 (C), 146.6 (C), 150.2 (2× C), 150.3 (4× C), 150.9 (2× C), 207.7 (6× C) ppm. MS (ES$^+$): *m*/*z* = 1173.0010 ($M^+$, $C_{61}H_{35}N_5O_6S_2{}^{56}Fe_2{}^{64}Zn$ requires 1173.0019), 1175 (100%), 1171 (10), 1172 (14), 1173 (84), 1174 (98), 1176 (80), 1177 (69), 1178 (49), 1179 (26), 1180 (13), 1181 (6). $C_{61}H_{35}N_5O_6S_2Fe_2Zn$ (1175.16): calcd. C 62.34, H 3.00, N 5.96; found C 62.45, H 3.70, N 5.72.

**[$Fe_2(CO)_6$(1,8-$S_2$-2-CH=*N*-(4-methoxyphenyl)-$C_{10}H_5$)] (2):** A solution of imine **8** (0.10 g, 0.31 mmol) and $Fe_3(CO)_{12}$ (0.16 g, 0.31 mmol) in toluene (8.0 mL) was refluxed for 2 h under argon atmosphere. The mixture was cooled down to room temperature, filtered and concentrated under reduced pressure. The residue was purified by column chromatography (8:2, hexane/EtOAc) to afford complex **2** as a bright orange solid (0.14 g, 76%). $R_f$ = 0.75 (8:2, hexane/EtOAc); mp: decomp. above 140 °C; $\lambda_{nm}$ ($CH_3CN$) 288 ($\varepsilon = 2.4\times10^4$ $M^{-1}$ $cm^{-1}$), 242 ($\varepsilon = 2.2\times10^4$ $M^{-1}$ $cm^{-1}$). IR (solid neat, ATR): $\tilde{\nu}_{max}$ = 2066 (CO), 2024 (CO), 1977 (CO), 1959 (CO) $cm^{-1}$. $^1$H NMR (400 MHz, $CDCl_3$): $\delta$ = 3.88 (s, 3 H, $OCH_3$), 7.02 (d, *J* = 8.7 Hz, 2 H, Ar*H*), 7.41–7.46 (m, 3 H, Ar*H*), 8.00 (app d, *J* = 8.5 Hz, 2 H, Ar*H*), 8.27 (d, *J* = 7.3 Hz, 1 H, Ar*H*), 8.41 (d, *J* = 8.5 Hz, 1 H, Ar*H*), 9.79 (s, 1 H, *H*C=N); $^{13}$C NMR (101 MHz, $CDCl_3$): 55.7 ($CH_3$), 114.7 (2× CH), 123.0 (2× CH), 125.2 (CH), 125.8 (C), 126.3 (CH), 126.6 (C), 127.5 (C), 131.3 (CH), 132.3 (CH), 133.6 (CH), 135.5 (C), 139.1 (C), 144.7 (C), 156.4 (CH), 159.2 (C), 207.5 (6× C) ppm. *m*/*z* (EI$^+$) 602.8836 ($M^+$, $C_{24}H_{13}NO_7S_2{}^{56}Fe_2$ requires 602.8832), 323 (100%), 308 (36), 435 (93, $M^+$ – 6 CO), 519 (72, $M^+$ – 3 CO), 603 (24) [$M^+$]. $C_{24}H_{13}NO_7S_2Fe_2$ (603.18): calcd. C 47.79, H 2.17, N, 2.32; found C 47.92, H 2.13, N 2.49.

**[$Fe_2(CO)_6$(1,8-$Se_2$-2-CH=*N*-(4-methoxyphenyl)-$C_{10}H_5$)] (3):** A solution of imine **9** (0.10 g, 0.24 mmol) and $Fe_3(CO)_{12}$ (0.12 g, 0.24 mmol) in toluene (6.2 mL) was refluxed for 1.5 h under argon atmosphere. The mixture was cooled down to room temperature, filtered and concentrated under reduced pressure. The residue was purified by column chromatography (8:2, hexane/EtOAc) to afford complex **3** as a red solid (0.10 g, 58%). $R_f$ = 0.86 (8:2, hexane/EtOAc); m.p. decomp. above 140 °C; $\lambda_{nm}$ ($CH_3CN$) 290 ($\varepsilon = 2.5\times10^4$ $M^{-1}$ $cm^{-1}$), 242 ($\varepsilon = 2.7\times10^4$ $M^{-1}$ $cm^{-1}$). IR (solid neat, ATR): $\tilde{\nu}_{max}$ = 2061 (CO), 2024 (CO), 1978 (CO), 1953 (CO) $cm^{-1}$. $^1$H NMR (400 MHz, $CDCl_3$): $\delta$ = 3.88 (s, 3 H, $OCH_3$), 7.03 (d, *J* = 8.0 Hz, 2 H, Ar*H*), 7.38–7.43 (m, 3 H, Ar*H*), 7.97 (app d, *J* = 8.5 Hz, 2 H, Ar*H*), 8.32 (d, *J* = 6.8 Hz, 1 H, Ar*H*), 8.38 (d, *J* = 8.5 Hz, 1 H, Ar*H*), 9.77 (s, 1 H, *H*C=N); $^{13}$C NMR (101 MHz, $CDCl_3$): 55.6 ($CH_3$), 114.6 (2× CH), 119.5 (C), 121.0 (C), 122.9 (2× CH), 125.3 (CH), 126.0 (CH), 129.5 (C), 131.7 (CH), 132.9 (CH), 135.0 (CH), 135.1 (C), 140.2 (C), 144.4 (C), 157.4 (CH), 159.1 (C), 208.2 (6× C) ppm. *m*/*z* (EI$^+$) 696.7180 ($M^+$, $C_{24}H_{13}NO_7{}^{56}Fe_2{}^{78}Se^{80}Se$ requires 696.7149), 557 (100%), 559 (78), 611 (9), 613 (35), 615 (35). $C_{24}H_{13}NO_7Fe_2Se_2$ (696.97): calcd. C 41.36, H 1.88, N 2.01; found C 39.09, H 2.14, N 2.11.

**[$Fe_2(CO)_6$(1,8-$S_2$-2-$CH_2$-*N*-(4-methoxyphenyl)-$C_{10}H_5$)] (4):** $NaBH_4$ (0.23 g, 6.20 mmol) was added in one portion to a solution of imine **8** (0.10 g, 0.31 mmol) in a mixture of MeOH/$CHCl_3$ (5:1, 15 mL) and the reaction was then stirred for 3 h at room temperature and under argon atmosphere. The resulting bright yellow solution was poured into $H_2O$ (51 mL) and the two layers were then separated. The aqueous layer was extracted with $CH_2Cl_2$ (3 × 20 mL). The combined organic layers were washed with brine (20 mL), dried with $MgSO_4$ and concentrated under reduced pressure to give the amine (0.10 g, 99%) as a pale yellow solid, which was used without further purification. A solution of the amine (0.10 g, 0.32 mmol) and $Fe_3(CO)_{12}$ (0.16 g, 0.32 mmol) in toluene (8.2 mL) was refluxed for 4 h under argon atmosphere. The mixture was cooled down to room temperature, filtered and concentrated under reduced pressure. The residue was purified by column chromatography (8:2, hexane/EtOAc) to afford complex **4** as a red solid (0.08 g, 39%). $R_f$ = 0.35 (8:2, hexane/EtOAc); m.p. decomp. above 150 °C. $\lambda_{nm}$ ($CH_3CN$) = 351 ($\varepsilon = 1.7\times10^4$ $M^{-1}$ $cm^{-1}$), 253 ($\varepsilon = 3.0\times10^4$ $M^{-1}$ $cm^{-1}$). IR (solid neat, ATR): $\tilde{\nu}_{max}$ = 2064 (CO), 2026 (CO), 2005 (CO), 1988 (CO), 1963 (CO) $cm^{-1}$. $^1$H NMR (400 MHz, $CDCl_3$): 3.72 (s, 3 H, $OCH_3$), 4.94 (2 H, $CH_2$), 6.61 (d, *J* = 8.1 Hz, 2 H, Ar*H*), 6.76 (d, *J* = 8.1 Hz, 2 H, Ar*H*), 7.37 (t, *J* = 7.8 Hz, 1 H, Ar*H*), 7.65 (d, *J* = 8.2 Hz, 1 H, Ar*H*), 7.91 (d, *J* = 8.2 Hz, 1 H, Ar*H*), 7.95 (d, *J* = 7.8 Hz, 1 H, Ar*H*), 8.25 (d, *J* = 7.8 Hz, 1 H, Ar*H*); $^{13}$C NMR: $\delta$ = (101 MHz, $CDCl_3$): 49.3 ($CH_2$), 55.9 ($CH_3$), 114.7 (2× CH), 115.1 (2× CH), 122.8 (C), 124.7 (C), 125.0 (CH), 126.8 (CH), 127.4 (C), 131.4 (CH), 132.3 (CH), 133.2 (CH), 133.7 (C), 141.7 (C), 143.9 (C), 152.7 (C), 207.7 (6× C) ppm. *m*/*z* (EI$^+$) 604.8994 ($M^+$, $C_{24}H_{15}NO_7{}^{56}Fe_2S_2$ requires 604.8989), 605 (100%), 606 (14). $C_{24}H_{15}NO_7Fe_2S_2$ (605.20): calcd. C 47.63, H 2.50, N 2.31; found C 47.75, H 2.44, N 2.45.

**[$Fe_2(CO)_6$(1,8-$Se_2$-2-$CH_2$-*N*-(4-methoxyphenyl)-$C_{10}H_5$)] (5):** $NaBH_4$ (0.18 g, 4.79 mmol) was added in one portion to a solution of imine **9** (0.10 g, 0.24 mmol) in a mixture of MeOH/$CHCl_3$ (5:1, 11 mL) and the reaction was then stirred for 3 h at room temperature under argon atmosphere. The resulting bright orange precipitate was poured into $H_2O$ (51 mL) and the two layers were then separated. The aqueous layer was extracted with $CH_2Cl_2$ (3 × 20 mL). The combined organic layers were washed with brine (20 mL), dried with $MgSO_4$ and concentrated under reduced pressure to give the amine (0.10 g, 99%) as a pale orange solid, which was used without further purification. A solution of the amine (0.10 g, 0.25 mmol) and $Fe_3(CO)_{12}$ (0.13 g, 0.24 mmol) in toluene (6.5 mL) was refluxed for 2.5 h under argon atmosphere. The mixture was cooled down to room temperature, filtered and concentrated under reduced pressure. The residue was purified by column chromatography (8:2, hexane/EtOAc) to afford complex **5** as a red crystalline solid (0.09 g, 52%). $R_f$ = 0.73 (8:2, hexane/EtOAc); m.p. decomp. above 150 °C. $\lambda_{nm}$ ($CH_3CN$) = 346 ($\varepsilon = 1.6\times10^4$ $M^{-1}$ $cm^{-1}$), 305 ($\varepsilon = 1.4\times10^4$ $M^{-1}$ $cm^{-1}$), 250 ($\varepsilon = 3.4\times10^4$ $M^{-1}$ $cm^{-1}$); IR (solid neat, ATR): $\tilde{\nu}_{max}$ = 2057 (CO), 2020 (CO), 1997 (CO), 1981 (CO), 1958 (CO) $cm^{-1}$. $^1$H NMR (500 MHz, $CDCl_3$): 3.73 (s, 3 H, $OCH_3$), 4.03 (1 H, N-H), 4.95 (2 H, $CH_2$), 6.61 (d, *J* = 8.8 Hz, 2 H, Ar*H*), 6.78 (d, *J* = 8.8 Hz, 2 H, Ar*H*), 7.34 (t, *J* = 7.6 Hz, 1 H, Ar*H*), 7.66 (d, *J* = 8.4 Hz, 1 H, Ar*H*), 7.86 (d, *J* = 8.4 Hz, 1 H, Ar*H*), 7.93 (d, *J* = 7.6 Hz, 1 H, Ar*H*), 8.29 (d, *J* = 7.6 Hz, 1 H, Ar*H*); $^{13}$C NMR = (125 MHz, $CDCl_3$): 51.3 ($CH_2$), 56.0 ($CH_3$), 114.6 (2× CH), 115.2 (2× CH), 118.2 (C), 118.9 (C), 124.9 (CH), 126.8 (CH), 129.7 (C), 131.9 (CH), 132.9 (CH), 133.5 (C), 134.8 (CH), 141.9 (C), 144.3 (C), 152.8 (C), 208.5 (6× C) ppm. MS (ES$^+$): *m*/*z* = 699.7958 ([M + H]$^+$, $C_{24}H_{16}NO_7{}^{56}Fe_2{}^{78}Se^{80}Se$ requires 699.7964), 702 (100%), 696 (14), 687 (10), 698 (50), 699 (28), 700 (99), 701 (20), 703 (16), 704 (19). $C_{24}H_{15}NO_7Fe_2Se_2$ (698.99): calcd. C 41.24, H 2.16, N 2.00; found C 39.49, H 2.00, N 2.30.

**(*E*)-*N*-(4-Methoxyphenyl)-1-(naphtho[1,8-*cd*][1,2]dithiol-3-yl)-methanimine (8):** A solution of aldehyde **6** (0.10 g, 0.46 mmol) and 4-methoxyaniline (1.10 g, 9.20 mmol) in dry $CH_3CN$ (10 mL) was

refluxed for 22 h under argon atmosphere. The reaction mixture was cooled down to room temperature and the solvent was removed under reduced pressure. Purification by column chromatography (toluene) gave imine **8** (0.15 g, 96%) as a bright orange crystalline solid. $R_f$ = 0.52 (toluene); m.p. 125–126 °C. IR (solid neat, ATR): $\tilde{\nu}_{max}$ = 3050, 2996, 2951, 2832, 1600, 1572, 1520, 1503, 1494, 1430, 1316, 1289, 1243, 1205, 1183, 1144, 1105, 1058, 1031, 966, 908, 823, 811, 777, 754, 733 $cm^{-1}$. $^1H$ NMR (400 MHz, $CDCl_3$): 3.85 (s, 3 H, $OCH_3$), 6.97 (d, $J$ = 8.5 Hz, 2 H, Ar*H*), 7.38 (d, $J$ = 8.5 Hz, 2 H, Ar*H*), 7.41–7.47 (m, 3 H, Ar*H*), 7.49 (d, $J$ = 8.3 Hz, 1 H, Ar*H*), 7.57 (d, $J$ = 8.3 Hz, 1 H, Ar*H*), 8.78 (s, 1 H, *H*C=N); $^{13}C$ NMR = (101 MHz, $CDCl_3$): 55.7 ($CH_3$), 114.8 (2× CH), 117.3 (CH), 120.4 (CH), 122.3 (2× CH), 126.4 (C), 128.1 (CH), 128.6 (CH), 135.7 (C), 135.8 (C), 141.5 (C), 146.7 (C), 148.6 (C), 151.8 (CH), 158.7 (C) ppm. MS ($ES^+$): $m/z$ = 323.0441 ($M^+$, $C_{18}H_{13}NOS_2$ requires 323.0439), 323 (100%), 324 (34), 325 (7). $C_{18}H_{13}NOS_2$ (323.43): calcd. C 66.84, H 4.05, N 4.33; found C 67.07, H 3.86, N 4.49.

**(*E*)-*N*-(4-Methoxyphenyl)-1-(naphtho[1,8-*cd*][1,2]diselenol-3-yl)-methanimine (9):** A solution of $TiCl_4$ (0.04 mL, 0.39 mmol) in dry $CH_2Cl_2$ (0.9 mL) was added dropwise over 10 min to a solution of aldehyde **7** (0.30 g, 0.96 mmol), 4-methoxyaniline (0.14 g, 1.15 mmol) and $NEt_3$ (0.27 mL, 1.92 mmol) in dry $CH_2Cl_2$ (7.9 mL) at 0 °C and under argon atmosphere. After 30 min the reaction mixture was warmed to room temperature and stirred for an additional 16 h. The solvent was removed under reduced pressure and the crude product was then purified by column chromatography (8:2, hexane/EtOAc) to give imine **9** (0.38 g, 94%) as a bright red crystalline solid. $R_f$ = 0.71 (8:2, hexane/EtOAc); mp: 124–125 °C. IR (solid neat, ATR): $\tilde{\nu}_{max}$ = 1598, 1562, 1504, 1432, 1419, 1288, 1243, 1182, 1108, 1029, 830, 813, 796, 756, 737 $cm^{-1}$. $^1H$ NMR (400 MHz, $CDCl_3$): $\delta$ = 3.86 (s, 3 H, $OCH_3$), 6.96–7.01 (m, 2 H, Ar*H*), 7.39 (d, $J$ = 7.7 Hz, 1 H, Ar*H*), 7.41–7.46 (m, 2 H, Ar*H*), 7.57 (d, $J$ = 7.7 Hz, 1 H, Ar*H*), 7.61 (d, $J$ = 8.4 Hz, 1 H, Ar*H*), 7.70 (d, $J$ = 8.4 Hz, 1 H, Ar*H*), 7.82 (d, $J$ = 7.7 Hz, 1 H, Ar*H*), 8.93 (s, 1 H, *H*C=N); $^{13}C$ NMR (101 MHz, $CDCl_3$): 55.7 ($CH_3$), 115.0 (2× CH), 121.9 (CH), 122.9 (2× CH), 124.6 (CH), 125.0 (CH), 127.6 (CH), 128.1 (CH), 129.9 (C), 137.0 (C), 138.5 (C), 139.8 (C), 145.8 (C), 151.4 (C), 151.8 (CH), 159.0 (C) ppm. MS ($ES^+$): $m/z$ = 417.9413 ([M + H]$^+$, $C_{18}H_{14}NO\ ^{78}Se^{80}Se$ requires 417.9414), 420 (100%), 413 (7), 414 (16), 415 (29), 416 (50), 417 (73), 418 (84), 419 (64), 421, (22), 422 (19).

**Zinc (*E*)-*N*-(TPP)-Naphtho[1,8-*cd*][1,2]dithiol-3-ylmethanimine (11):** $Zn(OAc)_2{\cdot}2H_2O$ (0.04 g, 0.17 mmol) was added in one portion to a solution of amine **10** (0.06 g, 0.09 mmol) in pyridine (13 mL) at room temperature and under argon atmosphere and the reaction mixture was refluxed for 1 h and after this time TLC analysis ($CH_2Cl_2$) indicated total consumption of **10** and formation of zinc amine **16**. The reaction mixture was cooled down to room temperature, added with aldehyde **6** (0.02 g, 0.09 mmol) and more $Zn(OAc)_2{\cdot}2H_2O$ (0.08 g, 0.35 mmol) and refluxed for 2 d. Pyridine was evaporated under reduced pressure and the residue purified by column chromatography ($CH_2Cl_2$) to give zinc imine **11** as a bright purple opaque solid (0.08 g, 96%). $R_f$ = 0.93 ($CH_2Cl_2$); m.p. decomp. above 200 °C. IR (solid neat, ATR): $\tilde{\nu}_{max}$ = 3051, 3020, 2988, 2970, 2921, 1596, 1569, 1518, 1485, 1438, 1339, 1316, 1206, 1170, 1069, 994, 967, 907, 814, 750, 729, 715, 701 $cm^{-1}$. $^1H$ NMR (400 MHz, [$D_6$]DMSO): $\delta$ = 7.58–7.63 (m, 1 H, Ar*H*), 7.69 (t, $J$ = 7.6 Hz, 2 H, Ar*H*), 7.77 (d, $J$ = 8.4 Hz, 1 H, Ar*H*), 7.79–7.92 (m, 9 H, Ar*H*), 7.93 (d, $J$ = 8.2 Hz, 2 H, Ar*H*), 8.00 ($J$ = 8.5 Hz, 1 H, Ar*H*), 8.17–8.23 (m, 6 H, Ar*H*), 8.29 (d, $J$ = 8.2 Hz, 2 H, Ar*H*), 8.78 (s, 4 H, Ar*H*), 8.81 (d, $J$ = 4.6 Hz, 2 H, Ar*H*), 8.90 (d, $J$ = 4.6 Hz, 2 H, Ar*H*), 9.55 (s, 1 H, Ar*H*); $^{13}C$ NMR (101 MHz [$D_6$]-DMSO) 117.7 (CH), 119.7 (2× C), 119.9 (2× CH), 120.4 (2× C), 120.7 (CH), 122.6 (CH), 126.4 (C), 126.6 (6× CH), 127.5 (3× CH), 129.1 (CH), 129.2 (CH), 131.7 (4× CH), 131.7 (4× CH), 134.2 (6× CH), 134.9 (2× C), 135.4 (2× CH), 141.2 (C), 142.8 (3× C), 145.8 (C), 146.8 (C), 147.8 (C), 149.3 (8× C), 155.4 (CH) ppm. MS ($ES^+$): $m/z$ = 892.1575 ([M + H]$^+$, $C_{55}H_{34}N_5S_2{}^{64}Zn$ requires 892.1547), 893 (100%), 891 (84), 892 (96), 894 (87), 895 (80), 896 (63), 897 (51), 898 (30), 900 (24).

**Zinc (*E*)-*N*-(TPP)-Naphtho[1,8-*cd*][1,2]diselenol-3-ylmethanimine (12):** $Zn(OAc)_2{\cdot}2H_2O$ (0.07 g, 0.33 mmol) was added in one portion to a solution of amine **16** (0.05 g, 0.07 mmol) and aldehyde **7** (0.02 g, 0.07 mmol) in pyridine (10 mL) at room temperature and under argon atmosphere and the reaction mixture was refluxed for 2 d. The reaction mixture was cooled down to room temperature and the solvent was evaporated under reduced pressure. The residue was purified by column chromatography ($CH_2Cl_2$) to give imine **12** as a bright purple opaque solid (0.04 g, 61%). $R_f$ = 0.94 ($CH_2Cl_2$); m.p. decomp. above 230 °C. IR (solid neat, ATR): $\tilde{\nu}_{max}$ = 3658, 2988, 2971, 2920, 2902, 1596, 1561, 1507, 1483, 1430, 1416, 1394, 1338, 1229, 1204, 1184, 1171, 1141, 1067, 1001, 993, 955, 814, 750, 728, 698 $cm^{-1}$. $^1H$ NMR (400 MHz, [$D_6$]DMSO): $\delta$ = 7.54 (t, $J$ = 8.0 Hz, 1 H, Ar*H*), 7.70 (d, $J$ = 8.0 Hz, 1 H, Ar*H*), 7.80–7.82 (m, 9 H, Ar*H*), 7.93–7.97 (m, 2 H, Ar*H*), 8.02 (d, $J$ = 8.0 Hz, 1 H, Ar*H*), 8.05 (d, $J$ = 8.2 Hz, 2 H, Ar*H*), 8.18–8.21 (m, 6 H, Ar*H*), 8.32 (d, $J$ = 8.2 Hz, 2 H, Ar*H*), 8.79 (s, 4 H, Ar*H*), 8.82 (d, $J$ = 4.6 Hz, 2 H, Ar*H*), 8.91 (d, $J$ = 4.6 Hz, 2 H, Ar*H*), 9.81 (s, 1 H, *H*C=N) ppm. $^{13}C$ NMR (101 MHz, [$D_6$]DMSO): $\delta$ = 119.5 (C), 120.2 (2× CH), 120.4 (2× C), 122.0 (CH), 123.9 (C), 124.3 (CH), 124.9 (CH), 126.6 (6× CH), 127.5 (3× CH), 128.5 (CH), 128.7 (CH), 130.3 (C), 131.5 (2× CH), 131.6 (4× CH), 131.7 (2× CH), 134.1 (6× CH), 135.6 (2× CH), 136.8 (C), 137.8 (C), 141.6 (C), 142.7 (3× C), 145.2 (C), 145.3 (C), 149.2 (2× C), 149.3 (4× C), 149.5 (2× C), 150.7 (C), 155.3 (CH) ppm. MS ($ES^+$): $m/z$ = 988.0437 ([M + H]$^+$, $C_{55}H_{34}N_5{}^{64}Zn\ ^{80}Se_2$ requires 988.0436), 988 (100%), 983 (31), 984 (48), 985 (66), 986 (82), 987 (86), 989 (78), 990 (73), 991 (56), 992 (43), 993 (24).

**(*E*)-*N*-(TPP)-Naphtho[1,8-*cd*][1,2]dithiol-3-ylmethanimine (13):** $La(OTf)_3$ (0.04 g, 0.06 mmol) was added in one portion to a solution of amine **10** (0.10 g, 0.16 mmol) and aldehyde **6** (0.05 g, 0.24 mmol) in dry toluene (20 mL) at room temperature and under argon atmosphere. The reaction mixture was refluxed for 8 h. Toluene was evaporated under reduced pressure and the residue purified by column chromatography ($CH_2Cl_2$) to give imine **13** as a purple crystalline solid (0.12 g, 87%). $R_f$ = 0.96 ($CH_2Cl_2$); m.p. >300 °C. IR (solid neat, ATR): $\tilde{\nu}_{max}$ = 3315, 1595, 1568, 1517, 1471, 1435, 1401, 1348, 1315, 1209, 1185, 1169, 1155, 1145, 1072, 1058, 981, 964, 905, 876, 795, 749, 720, 698 $cm^{-1}$. $^1H$ NMR (400 MHz, $CDCl_3$): $\delta$ = –2.73 (s, 2 H, inner *H*N), 7.16–7.22 (m, 1 H, Ar*H*), 7.25–7.29 (m, 1 H, Ar*H*), 7.50–7.54 (m, 3 H, Ar*H*), 7.56 (d, $J$ = 8.4 Hz, 2 H, Ar*H*), 7.71 (d, $J$ = 8.4 Hz, 2 H, Ar*H*), 7.73 (m, 9 H, Ar*H*), 8.22–8.27 (m, 4 H, Ar*H*), 8.27–8.32 (m, 2 H, Ar*H*), 8.87 (s, 4 H, Ar*H*), 8.89 (d, $J$ = 4.8 Hz, 2 H, Ar*H*), 8.95 (d, $J$ = 4.8 Hz, 2 H, Ar*H*), 9.15 (s, 1 H, *H*C=N); $^{13}C$ NMR (101 MHz, $CDCl_3$): 117.5 (CH), 119.7 (C), 120.0 (2× CH), 120.4 (3× C), 120.5 (CH), 122.5 (CH), 126.2 (C), 126.8 (6× CH), 127.9 (3× CH), 129.5 (CH), 129.0 (CH), 130.0–132.0 (br. peak, 8× CH), 134.7 (6× CH), 135.8 (2× CH), 136.0 (2× C), 140.6 (C), 142.3 (3× C), 146.9 (C), 148.0 (C), 149.5 (C), 154.3 (CH) ppm. C-α did not appear in the recorded $^{13}C$ NMR spectrum. MS ($ES^+$): $m/z$ = 830.2416 ([M + H]$^+$, $C_{55}H_{36}N_5S_2$ requires 830.2412), 830 (100%), 831 (64), 832 (26), 833 (9).

**(*E*)-*N*-(TPP)-Naphtho[1,8-*cd*][1,2]diselenol-3-ylmethanimine (14):** $La(OTf)_3$ (0.01 g, 0.01 mmol) was added in one portion to a solu-

tion of amine **10** (0.03 g, 0.05 mmol) and aldehyde **7** (0.03 g, 0.08 mmol) in toluene (6.7 mL) at room temperature and under argon atmosphere. The reaction mixture was heated under reflux and stirred for an additional 8 h. Toluene was removed under reduced pressure and the residue purified by column chromatography ($CH_2Cl_2$) to give imine **14** as a purple crystalline solid (0.04 g, 75%). $R_f$ = 0.95 ($CH_2Cl_2$); m.p. > 300 °C. IR (solid neat, ATR): $\tilde{\nu}_{max}$ = 3318, 2921, 2852, 1561, 1509, 1472, 1418, 1348, 1319, 1205, 1185, 1171, 1000, 982, 965, 847, 794, 763, 752, 719 $cm^{-1}$. $^1H$ NMR (400 MHz, $CDCl_3$): $\delta$ = –2.74 (s, 2 H, inner *H*N), 7.48 (t, *J* = 7.7 Hz, 1 H, Ar*H*), 7.65 (d, *J* = 7.7 Hz, 1 H, Ar*H*), 7.73–7.82 (m, 11 H, Ar*H*), 7.87 (d, *J* = 8.2 Hz, 2 H, Ar*H*), 7.90 (d, *J* = 7.5 Hz, 1 H, Ar*H*), 8.20–8.26 (m, 6 H, Ar*H*), 8.32 (d, *J* = 8.2 Hz, 2 H, Ar*H*), 8.86 (s, 4 H, Ar*H*), 8.89 (d, *J* = 4.8 Hz, 2 H, Ar*H*), 8.94 (d, *J* = 4.8 Hz, 2 H, Ar*H*), 9.33 (s, 1 H, *H*C=N); $^{13}C$ NMR (101 MHz, $CDCl_3$): 120.3 (2× CH), 120.4 (4× C), 122.1 (CH), 124.7 (CH), 125.3 (CH), 126.9 (6× CH), 127.9 (3× CH), 128.0 (CH), 128.4 (C), 128.5 (CH), 129.2 (C), 130.0 (C), 131.0–132.0 (br. peak, 8× CH), 136.7 (6× CH), 136.0 (2× CH), 137.4 (C), 141.1 (C), 142.3 (3× C), 146.2 (C), 146.3 (C), 154.0 (CH) ppm. C-α Pyrrole did not appear in the recorded $^{13}C$ NMR spectrum. MS ($ES^+$): *m*/*z* = 924.1331 ($[M + H]^+$, $C_{55}H_{36}N_5{}^{78}Se^{80}Se$ requires 924.1309), 926 (100%), 920 (15), 921 (21), 922 (52), 923 (57), 924 (82), 927 (54), 928 (37), 929 (12). $C_{55}H_{35}N_5Se_2$ (923.82): calcd. C 71.51, H 3.82, N 7.58; found C 70.38, H 4.01, N 7.09.

**TPP-*N*-(Naphtho[1,8-*cd*][1,2]dithiol-3-ylmethyl)aniline (15):** $NaBH_3CN$ (0.36 mL of a 1 M solution in THF, 0.36 mmol) was added dropwise to a solution of imine **13** (0.05 g, 0.06 mmol) in a mixture of THF/MeOH (1:1, 19 mL) at room temperature, followed by glacial AcOH (1 drop). The reaction mixture was heated under reflux for 8.5 h under argon atmosphere. The mixture was cooled down to room temperature, the solvent evaporated under reduced pressure and the residue purified by column chromatography (8:2, $CH_2Cl_2$/hexane to $CH_2Cl_2$) to give amine **15** as a purple crystalline solid (0.03 g, 65%). $R_f$ = 0.95 ($CH_2Cl_2$); mp: 183–184 °C. IR (solid neat, ATR): $\tilde{\nu}_{max}$ = 3316, 3051, 2954, 2921, 2853, 1607, 1543, 1519, 1470, 1440, 1402, 1349, 1326, 1298, 1254, 1221, 1183, 1156, 1072, 1054, 1032, 965, 877, 840, 815, 797, 723, 700 $cm^{-1}$. $^1H$ NMR (400 MHz, $CDCl_3$): $\delta$ = –2.74 (s, 2 H, inner *H*N), 4.44 (s, 1 H, *H*N), 4.58 (s, 2 H, $CH_2$), 7.01 (d, *J* = 8.4 Hz, 2 H, Ar*H*), 7.23 (dd, *J* = 7.3, 0.3 Hz, 1 H, Ar*H*), 7.31 (t, *J* = 7.7 Hz, 1 H, Ar*H*), 7.40 (dd, *J* = 8.0, 0.5 Hz, 1 H, Ar*H*), 7.43 (d, *J* = 8.4 Hz, 1 H, Ar*H*), 7.46 (d, *J* = 8.4 Hz, 1 H, Ar*H*), 7.69–7.82 (m, 9 H, Ar*H*), 8.01 (d, *J* = 8.4 Hz, 2 H, Ar*H*), 8.22 (dd, *J* = 7.5, 1.5 Hz, 6 H, Ar*H*), 8.83 (s, 6 H, Ar*H*), 8.93 (d, *J* = 4.4 Hz, 2 H, Ar*H*); $^{13}C$ NMR (101 MHz, $CDCl_3$): 48.5 ($CH_2$), 111.9 (2× CH), 116.3 (CH), 119.7 (C), 120.1 (2× C), 120.9 (C), 121.5 (CH), 122.7 (CH), 126.8 (9× CH), 127.7 (CH), 127.8 (CH), 128.5 (C), 130.0–132.5 (br. peak, 8× CH), 132.8 (C), 134.7 (6× CH), 135.3 (C), 135.9 (2× CH), 136.0 (C), 142.1 (C), 142.4 (C), 142.4 (2× C), 143.9 (C), 147.1 (C) ppm, C-α Pyrrole did not appear in the recorded $^{13}C$ NMR spectrum. MS ($ES^+$): *m*/*z* = 832.2565 ($[M + H]^+$, $C_{55}H_{38}N_5S_2$ requires 832.2569), 830 (100%), 831 (70), 832 (93), 833 (47), 834 (17).

**X-ray Crystallography:** Suitable crystals were selected and datasets were measured on an Agilent SuperNova diffractometer equipped with an Atlas detector for **2** ($\lambda_{Mo-K\alpha}$ = 0.71073 Å) and by the EPSRC UK National Crystallography Service[39] on a Rigaku AFC12 goniometer equipped with an enhanced sensitivity (HG) Saturn724+ detector mounted at the window of an FR-E+ SuperBright molybdenum rotating anode generator ($\lambda$ = 0.71075 Å, Mo-$K_\alpha$) with HF Varimax optics for **4**. Both instruments were equipped with an Oxford Cryosystems Cryostream device with diffraction data collected at 100 K in all cases. An absorption correction was applied using CrysAlisPro[42] using a numerical absorption correction based on gaussian integration over a multifaceted crystal model for **2**. An empirical absorption correction was applied using CrystalClear-SM Expert[43] for **4**. Both structures were solved by direct methods in SHELXS-2014[44] and were refined by a full-matrix least-squares procedure on $F^2$ in SHELXL-2014.[44] All non-hydrogen atoms were refined with anisotropic displacement parameters. The hydrogen atoms were added at calculated positions and refined by use of a riding model with isotropic displacement parameters based on the equivalent isotropic displacement parameter ($U_{eq}$) of the parent atom. Figures were produced and some structural analysis was carried out using OLEX2.[45]

**2:** The structure contains two crystallographically-independent molecules. These are connected via a π-π stacking interaction between the naphthalene groups C(1)–C(10) and C(101)–C(110), with the angle between the least-squares planes through the atoms being 2.6 (2)° and the perpendicular distance between the plane through C(1)–C(10) and the centroid of the plane through C(101)–C(110) being 3.264 (7) Å (see Figure S4).

**4:** The crystal was the best quality that could be grown but the diffraction pattern was subject to streaking and as such the refinement is somewhat poor.

**X-ray Crystal Data for 2:** $C_{24}H_{13}Fe_2NO_7S_2$, *M* = 603.17, crystal dimensions: 0.234 × 0.067 × 0.020 mm, triclinic, *a* = 7.5048(3), *b* = 16.4362(8), *c* = 20.4236(14) Å, *α* = 92.017(5), *β* = 94.220(5), *γ* = 95.982(4)°, *U* = 2496.4(2) $Å^3$, space group $P\bar{1}$, *Z* = 4, $\rho_{calcd.}$ = 1.605 $g\,cm^{-3}$, $2\theta_{max}$ = 50.7°, $\mu$ = 1.374 $mm^{-1}$, max./min. transmission factors: 0.993/0.963. 23664 reflections measured, 9108 unique ($R_{int}$ = 0.0674) which were used in all calculations, 651 parameters. The final *R*1 was 0.0834 [$I > 2\sigma(I)$] and *wR*($F_2$) was 0.2490 (all data), max./min. residual electron density: 1.189/–1.349 e $Å^3$.

**X-ray Crystal Data for 4:** $C_{24}H_{15}Fe_2NO_7S_2$, *M* = 605.19, crystal dimensions: 0.09 × 0.01 × 0.01 mm, triclinic, *a* = 7.4381(6), *b* = 12.1808(9), *c* = 13.5281(10) Å, *α* = 96.12(3), *β* = 101.11(3), *γ* = 91.80(3)°, *U* = 1194.1(2) $Å^3$, space group $P\bar{1}$, *Z* = 2, $\rho_{calcd.}$ = 1.683 $g\,cm^{-3}$, $2\theta_{max}$ = 50.056°, $\mu$ = 1.436 $mm^{-1}$, max./min. transmission factors: 1.000/0.545, 8368 reflections measured, 4050 unique ($R_{int}$ = 0.1722) which were used in all calculations, 325 parameters. The final *R*1 was 0.1459 [$I > 2\sigma(I)$] and *wR*($F_2$) was 0.4021 (all data), max./min. residual electron density: 2.386/–0.805 e $Å^3$.

**Electrochemistry:** Electrochemical studies were performed with a CHI601B Electrochemical Analyzer. All measurements were carried out under argon at room temperature in dry $CH_3CN$, with the exception of **1**, where a mixed solvent system of $CH_2Cl_2$/$CH_3CN$ (7:3) was used because complex **1** is not soluble in acetonitrile, while $AgNO_3$ (the reference electrode) is not soluble in $CH_2Cl_2$. Tetrabutylammoniun hexafluorophosphate ($NBu_4PF_6$, 0.1 M in $CH_3CN$) was used as supporting electrolyte. A conventional 3-electrode system was employed. The working electrode was a glassy carbon electrode (diameter: 1.0 mm). Silver/silver nitrate (Ag/$AgNO_3$, 10 mM solution in $CH_3CN$) was used as an external reference electrode and a platinum wire was used as auxiliary electrode. Ferrocene was used as an internal reference. All potentials reported in this work are with reference to the $Fc/Fc^+$ couple. Cyclic voltammograms were recorded at a scan rate of 0.01 $V\,s^{-1}$. The range –0.8 V to –2.5 V, focusing on the wave, was also recorded at sweep rates between 0.01 $V\,s^{-1}$ to 0.2 $V\,s^{-1}$, although the capacitive current of the carbon substrate was rather high at the higher sweep rates.

All glassware was cleaned using a 1:1 mixture of ammonia and hydrogen peroxide followed by thorough rinsing with pure water.

 

Glassware was soaked in pure water for 12 h and then rinsed and oven-dried overnight. Water used throughout (including solution preparation and rinsing) was purified by a Millipore™ system (resistivity 18.2 MΩ cm, TOC ≤ 5 ppb). The working electrode was prepared by polishing with aqueous slurries of successively finer grades of alumina powder (1 μm, 0.3 μm and 0.05 μm, Buehler), followed by rinsing and placing in pure water in an ultrasonic bath for several minutes, then dried in a stream of argon.

## Acknowledgments

The authors thank the Engineering and Physical Sciences Research Council (EPSRC) and the University of Birmingham for funding. The NMR spectrometers used in this research were obtained through Birmingham Science City: Innovative Uses for Advanced Materials in the Modern World (West Midlands Centre for Advanced Materials Project 2), with financial support from the Advantage West Midlands (AWM) and part-funded by the European Regional Development Fund (ERDF). The authors thank the EPSRC UK National Crystallography Service at the University of Southampton for the collection of the crystallographic data for compound **4**.[39]

[1] a) H. Audus, O. Kaarstad, M. Kowal, *Decarbonisation of fuels: hydrogen as an energy carrier*, in: *Proceedings of the 11th World Hydrogen Energy Conference*, Stuttgart, Germany, June 23–28, **1996**, 525–534; b) T. N. Veziroglu, *Int. J. Hydrogen Energy* **2000**, *25*, 1143–1150; c) M. Momirlan, T. N. Veziroglu, *Renewable Sustainable Energy Rev.* **2002**, *6*, 141–179.

[2] a) L. M. Gandía, G. Arzamendi, P. M. Diéguez, in: *Renewable Hydrogen Energy: An Overview*, in: *Renewable Hydrogen Technologies*, Elsevier, **2013**, p. 1–17; b) A. J. Esswein, D. G. Nocera, *Chem. Rev.* **2007**, *107*, 4022–4047; c) J. D. Holladay, J. Hu, D. L. King, Y. Wang, *Catal. Today* **2009**, *139*, 244–260.

[3] a) L. Hammarström, S. Hammes-Schiffer, *Acc. Chem. Res.* **2009**, *42*, 1859–1860; b) M. R. Dubois, D. L. Dubois, *Acc. Chem. Res.* **2009**, *42*, 1974–1982; c) M. Wang, L. Chen, L. Sun, *Energy Environ. Sci.* **2012**, *5*, 6763–6778; d) V. S. Thoi, Y. Sun, J. R. Long, C. J. Chang, *Chem. Soc. Rev.* **2013**, *42*, 2388–2400.

[4] a) S. Losse, J. G. Vos, S. Rau, *Coord. Chem. Rev.* **2010**, *254*, 2492–2504; b) V. Artero, M. Chavarot-Kerlidou, M. Fontecave, *Angew. Chem. Int. Ed.* **2011**, *50*, 7238–7266; c) C. Bachmann, B. Probst, M. Guttentag, R. Alberto, *Chem. Commun.* **2014**, *50*, 6737–6739.

[5] a) S. Canaguier, V. Artero, M. Fontecave, *Dalton Trans.* **2008**, 315–325; b) M. R. DuBois, D. L. DuBois, *Acc. Chem. Res.* **2009**, *42*, 1974–1982; c) D. L. DuBois, M. R. Bullock, *Eur. J. Inorg. Chem.* **2011**, 1017–1027; d) Z. Han, F. Qiu, R. Eisenberg, P. L. Holland, T. D. Krauss, *Science* **2012**, *338*, 1321–1324; e) W. J. Shaw, M. L. Helm, D. L. DuBois, *Biochim. Biophys. Acta Bioenerg.* **2013**, *1827*, 1123–1139.

[6] H. I. Karunadasa, C. J. Chang, J. R. Long, *Nature* **2010**, *464*, 1329–1333.

[7] a) I. Bhugun, D. Lexa, J.-M. Saveant, *J. Am. Chem. Soc.* **1996**, *118*, 3982–3983; b) M. J. Rose, H. B. Gray, J. R. Winkler, *J. Am. Chem. Soc.* **2012**, *134*, 8310–8313; c) S. Kaur-Ghumaan, L. Schwartz, R. Lomoth, M. Stein, S. Ott, *Angew. Chem. Int. Ed.* **2010**, *49*, 8033–8036.

[8] a) M. Frey, *ChemBioChem* **2002**, *3*, 153–160; b) J.-C. Fontecilla-Camps, A. Volbeda, C. Cavazza, Y. Nicolet, *Chem. Rev.* **2007**, *107*, 4273–4303.

[9] For reviews on hydrogenases, see: a) K. A. Vincent, A. Parkin, F. A. Armstrong, *Chem. Rev.* **2007**, *107*, 4366–4413; b) W. Lubitz, H. Ogata, O. Rüdiger, E. Reijerse, *Chem. Rev.* **2014**, *114*, 4081–4148.

[10] a) J. W. Peters, W. N. Lanzillotta, B. J. Lemon, L. C. Seefeldt, *Science* **1998**, *282*, 1853–1858; b) Y. Nicolet, C. Piras, P. Legrand, C. E. Hatchikian, J.-C. Fontecilla-Camps, *Structure* **1999**, *7*, 13–23.

[11] a) J.-F. Capon, F. Gloaguen, P. Schollhammer, J. Talarmin, *Coord. Chem. Rev.* **2005**, *249*, 1664–1676; b) J.-F. Capon, F. Gloaguen, F. Y. Pétillion, P. Schollhammer, J. Talarmin, *Coord. Chem. Rev.* **2009**, *253*, 1476–1494; c) F. Gloaguen, T. B. Rauchfuss, *Chem. Soc. Rev.* **2009**, *38*, 100–108; d) C. Tard, C. J. Pickett, *Chem. Rev.* **2009**, *109*, 2245–2274; e) S. Tschierlei, S. Ott, R. Lomoth, *Energy Environ. Sci.* **2011**, *4*, 2340–2352; f) M. Y. Darensbourg, W. Weigand, *Eur. J. Inorg. Chem.* **2011**, 994–1004; g) T. R. Simmons, G. Berggren, M. Bacchi, M. Fontecave, V. Artero, *Coord. Chem. Rev.* **2014**, *270–271*, 127–150.

[12] C. Figliola, L. Male, P. N. Horton, M. B. Pitak, S. J. Coles, S. L. Horswell, R. S. Grainger, *Organometallics* **2014**, *33*, 4449–4460.

[13] a) J.-F. Capon, F. Gloaguen, P. Schollhammer, J. Talarmin, *J. Electroanal. Chem.* **2004**, *566*, 241–247; b) J.-F. Capon, F. Gloaguen, P. Schollhammer, J. Talarmin, *J. Electroanal. Chem.* **2006**, *595*, 47–52; c) L. Schwartz, P. S. Singh, L. Eriksson, R. Lomoth, S. Ott, *C. R. Chim.* **2008**, *11*, 875–889; d) L. Schwartz, L. Eriksson, R. Lomoth, F. Teixidor, C. Viñas, S. Ott, *Dalton Trans.* **2008**, 2379–2381; e) P. S. Singh, H. C. Rudbeck, P. Huang, S. Ezzaher, L. Eriksson, M. Stein, S. Ott, R. Lomoth, *Inorg. Chem.* **2009**, *48*, 10883–10885; f) R. J. Wright, C. Lim, T. D. Tilley, *Chem. Eur. J.* **2009**, *15*, 8518–8525; g) C. A. Mebi, B. C. Noll, R. Gao, D. Karr, *Z. Anorg. Allg. Chem.* **2010**, *636*, 2550–2554; h) J. Chen, A. K. Vanucci, C. A. Mebi, N. Okumura, S. C. Borowski, M. Swenson, L. T. Lockett, D. H. Evans, R. S. Glass, D. L. Lichtenberger, *Organometallics* **2010**, *29*, 5330–5340; i) D. Streich, M. Karnahl, Y. Astuti, C. W. Cady, L. Hammarström, R. Lomoth, S. Ott, *Eur. J. Inorg. Chem.* **2011**, 1106–1111; j) C. Topf, U. Monkowius, G. Knör, *Inorg. Chem. Commun.* **2012**, *21*, 147–150; k) E. S. Donovan, J. J. McCormick, G. S. Nichol, G. A. N. Felton, *Organometallics* **2012**, *31*, 8067–8070.

[14] For a review see: M. K. Harb, U.-P. Apfel, T. Sakamoto, M. El-khateeb, W. Weigand, *Eur. J. Inorg. Chem.* **2011**, 986–993. For more recent articles see: a) M. K. Harb, J. Windhager, T. Niksch, H. Görls, T. Sakamoto, E. R. Smith, R. S. Glass, D. L. Lichtenberger, D. H. Evans, M. Elkhateeb, W. Weigand, *Tetrahedron* **2012**, *68*, 10592–10599; b) L.-C. Song, Q.-L. Li, Z.-H. Feng, X.-J. Sun, Z.-J. Xie, H.-B. Song, *Dalton Trans.* **2013**, *42*, 1612–1626; c) L.-C. Song, B. Gai, Z.-H. Feng, Z.-Q. Du, Z.-J. Xie, X.-J. Sun, H.-B. Song, *Organometallics* **2013**, *32*, 3673–3684; d) R. Trautwein, L. R. Almazahreh, H. Görls, W. Weigand, *Z. Anorg. Allg. Chem.* **2013**, *639*, 1512–1519.

[15] a) L. Sun, B. Åkermark, S. Ott, *Coord. Chem. Rev.* **2005**, *249*, 1653–1663; b) M. Wang, Y. Na, M. Gorlov, L. Sun, *Dalton Trans.* **2009**, 6458–6467; c) R. Lomoth, S. Ott, *Dalton Trans.* **2009**, 9952–9959; d) M. Wang, L. Chen, X. Li, L. Sun, *Dalton Trans.* **2011**, *40*, 12793–12800; e) M. Wang, W.-G. Wang, H.-Y. Wang, G. Si, C.-H. Tung, L.-Z. Wu, *ACS Catal.* **2012**, *2*, 407–416; f) R. Goy, U.-P. Apfel, C. Elleouet, D. Escudero, M. Elstner, H. Görls, J. Talarmin, P. Shollhammer, L. Gonzalez, W. Weigand, *Eur. J. Inorg. Chem.* **2013**, 4466–4472; g) S. Gao, S. Huang, Q. Duan, J. Hou, D. Jiang, Q. Liang, J. Zhao, *Int. J. Hydrogen Energy* **2014**, *39*, 10434–10444.

[16] a) A. P. S. Samuel, D. T. Co, C. L. Stern, M. R. Wasielewski, *J. Am. Chem. Soc.* **2010**, *132*, 8813–8815; b) P. Poddutoori, D. T. Co, A. P. S. Samuel, C. H. Kim, M. T. Vagnini, M. R. Wasielewski, *Energy Environ. Sci.* **2011**, *4*, 2441–2450.

[17] a) R. S. Grainger, A. Procopio, J. W. Steed, *Org. Lett.* **2001**, *3*, 3565–3568; b) R. S. Grainger, B. Patel, B. M. Kariuki, *Angew. Chem. Int. Ed.* **2009**, *48*, 4832–4835; *Angew. Chem.* **2009**, *121*, 4926; c) R. S. Grainger, B. Patel, B. M. Kariuki, L. Male, N. Spencer, *J. Am. Chem. Soc.* **2011**, *133*, 5843–5852; d) B. Patel, J. Carlisle, S. E. Bottle, G. R. Hanson, B. M. Kariuki, L. Male, J. C. McMurtrie, N. Spencer, R. S. Grainger, *Org. Biomol. Chem.* **2011**, *9*, 2336–2344; e) S. Allenmark, R. S. Grainger, S. Olsson, B. Patel, *Eur. J. Org. Chem.* **2011**, 4089–4092.

[18] For reviews on the synthesis and application, including metal coordination chemistry, of 1,8-*peri*-substituted naphthalene dichalcogenides and related systems, see: a) P. Kilian, F. R. Knight, J. D. Woollins, *Coord. Chem. Rev.* **2011**, *255*, 1387–1413; b) P. Kilian, F. R. Knight, J. D. Woollins, *Chem. Eur. J.* **2011**, *17*, 2302–2328.
[19] a) G. Berggren, A. Adamska, C. Lambertz, T. R. Simmons, J. Esselborn, M. Atta, S. Gambarelli, J. M. Mouesca, E. Reijerse, W. Lubits, T. Happe, V. Artero, M. Fontecave, *Nature* **2013**, *499*, 66–69; b) J. Esselborn, C. Lambertz, A. Adamska-Venkatesh, T. R. Simmons, G. Berggren, J. Noth, J. Siebel, A. Hemschemeier, V. Artero, E. Reijerse, M. Fontecave, W. Lubitz, T. Happe, *Nat. Chem. Biol.* **2013**, *9*, 607–609.
[20] E. W. Miller, S. X. Bian, C. J. Chang, *J. Am. Chem. Soc.* **2007**, *129*, 3458–3459.
[21] D. Manna, G. Mugesh, *J. Am. Chem. Soc.* **2012**, *134*, 4269–4279.
[22] M. Periasamy, G. Srinivas, P. Bharathi, *J. Org. Chem.* **1999**, *64*, 4204–4205.
[23] This approach is not limited to aromatic amines. A similar sequence has been used to prepare *N*-isopropylamine-substituted [FeFe] complexes. See supporting information for details about synthesis and characterization.
[24] A. Adler, F. R. Longo, J. D. Finarelli, J. Goldmacher, J. Assour, L. Korsakoff, *J. Org. Chem.* **1967**, *32*, 476–476.
[25] W. J. Kruper Jr., T. A. Chamberlin, M. Kochanny, *J. Org. Chem.* **1989**, *54*, 2753–2756.
[26] L. Sun, H. Chen, Z. Zhang, Q. Yang, H. Tong, A. Xu, C. Wang, *J. Inorg. Biochem.* **2012**, *108*, 47–52.
[27] P. Rothemund, A. R. Menotti, *J. Am. Chem. Soc.* **1948**, *70*, 1808–1812.
[28] S. Sharma, M. Nath, *Beilstein J. Org. Chem.* **2013**, *9*, 496–502.
[29] Y.-J. Cho, T. K. Ahn, H. Song, K. S. Kim, C. Y. Lee, W. S. Seo, K. Lee, S. K. Kim, D. Kim, J. T. Park, *J. Am. Chem. Soc.* **2005**, *127*, 2380–2381.
[30] H. F. Visher, J. W. Hulshof, S. Hulscher, S. A. Fratantoni, M. H. P. Verheij, J. Victorina, M. J. Smit, I. J. P. de Esch, R. Leurs, *Bioorg. Med. Chem.* **2010**, *18*, 675–688.
[31] M. Hernández-Juárez, M. Vaquero, E. Álvarez, V. Salazar, A. Suárez, *Dalton Trans.* **2013**, *42*, 351–354.
[32] C. F. Works, *J. Chem. Educ.* **2007**, *84*, 836–838.
[33] CCDC-1031027 (for **2**) and -1031028 (for **4**) contain the supplementary crystallographic data for this paper. These data can be obtained free of charge from The Cambridge Crystallographic Data Centre via www.ccdc.cam.ac.uk/data_request/cif.
[34] G. A. N. Felton, R. S. Glass, D. L. Lichtenberger, D. H. Evans, *Inorg. Chem.* **2006**, *45*, 9181–9184.
[35] S. Ott, M. Kritikos, B. Åkermark, L. Sun, R. Lomoth, *Angew. Chem. Int. Ed.* **2004**, *43*, 1006–1009; *Angew. Chem.* **2004**, *116*, 1024.
[36] J. Hou, X. Peng, J. Liu, Y. Gao, X. Zhao, S. Gao, K. Han, *Eur. J. Inorg. Chem.* **2006**, 4679–4686.
[37] T. Liu, M. Wang, Z. Shi, H. Cui, W. Dong, J. Chen, B. Åkermark, L. Sun, *Chem. Eur. J.* **2004**, *10*, 4474–4479.
[38] a) L.-C. Song, M.-T. Tang, F.-H. Su, Q.-M. Hu, *Angew. Chem. Int. Ed.* **2006**, *45*, 1130–1133; *Angew. Chem.* **2006**, *118*, 1148; b) L.-C. Song, M.-T. Tang, S.-Z. Mei, J.-H. Huang, Q.-M. Hu, *Organometallics* **2007**, *26*, 1575–1577; c) L.-C. Song, L.-X. Wang, B.-S. Yin, Y.-L. Li, X.-G. Zhang, Y.-W. Zhang, X. Luo, Q.-M. Hu, *Eur. J. Inorg. Chem.* **2008**, 291–297; d) L.-C. Song, L.-X. Wang, C.-G. Li, F. Li, Z. Chen, *J. Organomet. Chem.* **2014**, *749*, 120–128; e) X. Li, M. Wang, S. Zhang, J. Pan, Y. Na, J. Liu, B. Åkermark, L. Sun, *J. Phys. Chem. B* **2008**, *112*, 8198–8202; f) A. M. Kluwer, R. Kapre, F. Hartl, M. Lutz, A. L. Spek, A. M. Brouwer, P. W. N. M. van Leeuwen, J. N. H. Reek, *Proc. Natl. Acad. Sci. USA* **2009**, *106*, 10460–10465; g) L.-C. Song, L.-X. Wang, M.-Y. Tang, C.-G. Li, H.-B. Song, Q.-M. Hu, *Organometallics* **2009**, *28*, 3834–3841.
[39] S. J. Coles, P. A. Gale, *Chem. Sci.* **2012**, *3*, 683–689.
[40] W. L. Armarego, D. D. Perrin, *Purification of Laboratory Chemicals*, Butterworth-Heinemann, Oxford, UK, 4th ed., **1998**.
[41] G. R. Fulmer, A. J. M. Miller, N. H. Sherden, H. E. Gottlieb, A. N. Nudelman, B. M. Stoltz, J. E. Bercaw, K. I. Goldberg, *Organometallics* **2010**, *29*, 2176–2179.
[42] *CrysAlisPro*, version 1.171.37.33c, *Agilent Technologies*, **2014**.
[43] *CrystalClear-SM Expert*, v. 3.1 b27, **2012**, Rigaku.
[44] G. M. Sheldrick, *Acta Crystallogr., Sect. A* **2008**, *64*, 112–122.
[45] O. V. Dolomanov, L. J. Bourhis, R. J. Gildea, J. A. K. Howard, H. Puschmann, *J. Appl. Crystallogr.* **2009**, *42*, 339–341.

Received: April 8, 2015
Published Online: June 12, 2015

 